

# MEMS-BASED THICK FILM PZT VIBRATIONAL ENERGY HARVESTER

*A. Lei<sup>1</sup>, R. Xu<sup>1</sup>, A. Thyssen<sup>1</sup>, A.C. Stoot<sup>1</sup>, T. L. Christiansen<sup>1</sup>, K. Hansen<sup>2</sup>, R. Lou-Møller<sup>2</sup>, E.V. Thomsen<sup>1</sup> and K. Birkelund<sup>1</sup>*

<sup>1</sup>Department of Micro- and Nanotechnology, Technical University of Denmark, DTU Nanotech, Building 345 East, DK-2800 Kongens Lyngby, Denmark

<sup>2</sup>Meggitt A/S, Hejreskovvej 18A, DK-3490 Kvistgaard, Denmark

## ABSTRACT

We present a MEMS-based unimorph silicon/PZT thick film vibrational energy harvester with an integrated proof mass. We have developed a process that allows fabrication of high performance silicon based energy harvesters with a yield higher than 90%. The process comprises a KOH etch using a mechanical front side protection of an SOI wafer with screen printed PZT thick film. The fabricated harvester device produces 14.0  $\mu\text{W}$  with an optimal resistive load of 100  $\text{k}\Omega$  from 1g ( $g=9.81 \text{ m s}^{-2}$ ) input acceleration at its resonant frequency of 235 Hz.

## INTRODUCTION

With the development in low power electronics, wireless sensor systems powered by batteries are now applicable in monitoring of e.g. machine and structures. However, the limited lifespan of electrochemical batteries requires periodical replacement for long term operation. For sensors located remotely or inaccessible, this might not be an option, instead larger batteries can be used but this severely compromises the total size of the sensor system. In order to realize long term autonomous wireless sensor systems, much effort has recently been put into the research and development of small scale energy scavenging devices that transforms excess ambient energy into electrical energy. Among the most common ambient sources of energy are thermal, mechanical or unused RF energy [1]. Harvesting of mechanical energy from vibrations usually employs an electrostatic, electromagnetic or piezoelectric transduction mechanism [2]. A piezoelectric transduction device normally consists of an elastic cantilever supporting a piezoelectric layer with metal electrodes on either side. The most common piezoelectric material used is PZT (lead zirconate titanate). PZT can be integrated with an elastic cantilever by either bulk processing or deposition.

Several energy harvesters with bulk PZT have been presented in literature [3], [4]. These harvesters are characterized by having large dimensions, since bulk processing defines some lower limits of feasible processing, hence compromising the incorporation in small sensor systems. Piezoelectric films can also be deposited using sputtering [5], plasma-enhanced chemical vapour deposition (PECVD) [6], sol-gel spin-on [7] or screen printing [8]. Common for the deposition methods are that they can be integrated with MEMS fabrication technologies, enabling small scale devices, well proven fabrication processes, low fabrication costs and high volume production. So far, the majority of MEMS-based vibrational energy harvesters

presented [7], [9], have been fabricated using the sol-gel spin-on method, limiting the PZT layer thickness to a few  $\mu\text{m}$ . To obtain a sufficiently powerful energy harvester, it is however desirable to use thicker PZT films [10], [11].

In this work we present a unimorph MEMS-based PZT thick film vibrational energy harvester fabricated by combining silicon etching in potassium hydroxide (KOH) using a mechanical front side protection as proposed by [9], a silicon-on-insulator (SOI) wafer to accurately define the thickness of the silicon part of the cantilever also used by [7] and the silicon compatible PZT thick film screen-printing technique presented by [8]. The developed process allows fabrication of high performance silicon based energy harvesters using standard MEMS processes with a yield higher than 90%. The piezoelectric ceramic used is InSensor® TF2100, which has a high coupling coefficient, making it preferable for the MEMS based energy harvesters.

## FABRICATION

The unimorph vibrational energy harvester is fabricated using a four mask fabrication process on a 4 inch (100 mm) silicon SOI wafer with a 20  $\mu\text{m}$  device layer, a 1  $\mu\text{m}$  buried oxide layer and a 500  $\mu\text{m}$  thick substrate (Figure 1(a)). A 1  $\mu\text{m}$  silicon oxide layer is thermally grown followed by a deposition of 170 nm stoichiometric LPCVD silicon nitride (Figure 1(b)). Backside openings in the nitride for the KOH etch are defined using UV lithography followed by RIE etching and the front side nitride is removed in a RIE etch (Figure 1(c)). Using UV lithography, e-beam deposition and lift-off, a bottom electrode consisting of a 50 nm titanium adhesion layer and a 500 nm platinum layer, also serving as a diffusion barrier [12], is defined (Figure 1(d)). On top of the bottom electrode a 15  $\mu\text{m}$  PZT thick film is deposited using screen printing (Figure 1(e)). Before the sintering, the PZT thick film is high pressure treated. As top electrode, a 400 nm gold layer is deposited by e-beam evaporation through a shadow mask (Figure 1(f)). The wafer is placed in a mechanical holder that protects the front side of the wafer but exposes the backside. The oxide is removed in a BHF solution, and the cavities are etched in a KOH solution where the buried oxide functions as an etch stop layer (Figure 1(g)). The PZT structures are covered with resist and the cantilevers are released by an oxide etch in BHF followed by a silicon etch using RIE (Figure 1(h)). The PZT thick film is polarized by applying an electric field between the top and bottom electrodes at an elevated temperature. A final energy harvesting device with the dimensions listed in Table 1 is seen in Figure 2.

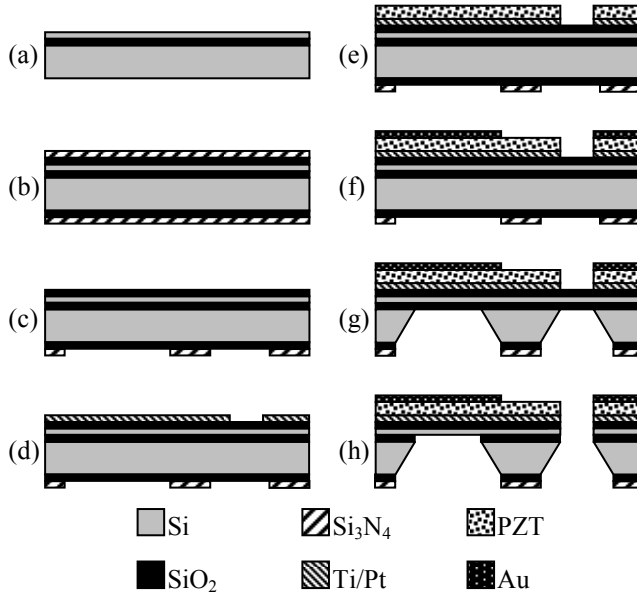


Figure 1: Process flow for the unimorph MEMS-based PZT thick film vibrational energy harvester.

Table 1: Dimensions of the energy harvester

Frame dimensions	10 mm × 10 mm
Medial dimension	< 1 mm
Cantilever width	5.5 mm
Cantilever length	1.95 mm
Mass length	4.55 mm
Mass width	5.5 mm

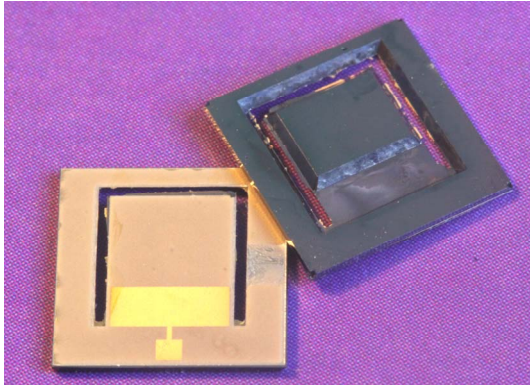


Figure 2: Photograph showing both sides of a fabricated energy harvesting device.

## RESULTS

The fabricated energy harvester is characterized by measuring the direct piezoelectric effect using a shaker setup to simulate the excess vibration noise from the surroundings, and the indirect piezoelectric effect using an Agilent 4294A Precision Impedance Analyzer to excite the harvester electrically.

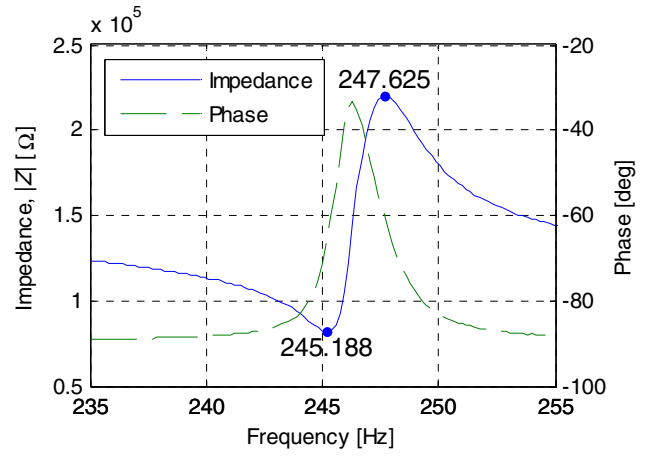


Figure 3: Impedance and phase around resonance. Source voltage set to 500 mV.

From the impedance measurement the resonant frequency, the capacitance, the optimal resistive load and the electromechanical coupling coefficient is determined. The resonance,  $f_r=245.2$  Hz and anti-resonance,  $f_a=247.6$  Hz is shown in Figure 3. The impedance at resonance is the optimal load resistance,  $R_{opt}=81.8$  k $\Omega$ . The coupling coefficient is found to be  $k=0.155$  and is calculated using

$$k = \sqrt{\frac{\alpha}{\alpha - \tan \alpha}}, \quad (1)$$

where,

$$\alpha = \frac{\pi f_a}{2 f_r}. \quad (2)$$

For the shaker measurements the harvester is being actuated by a B&K Mini Shaker 4810 driven by an amplified sinusoidal signal from a function generator. The acceleration is measured with a B&K Piezoelectric Accelerometer 8305. The applied input acceleration is stated in fractions of the gravitational acceleration  $g$  ( $9.81 \text{ m s}^{-2}$ ). From these measurements the resonant frequency and the optimal resistive load is confirmed. Furthermore, the power dissipated in a resistive load for different frequencies and accelerations is found.

The optimal resistive load for the energy harvester is found by extracting the RMS voltage from a resonant peak in a frequency sweep for various resistive loads at an input acceleration of  $0.5g$ . The power dissipated in the load will then be,  $P=V_{rms}^2/R_{Load}$ . The optimal resistive load, resulting in the highest power at resonance frequency, is found to 100 k $\Omega$ , see Figure 4. The increase in the optimal resistive load compared to the impedance measurement in Figure 3 is due to increased mechanical damping associated with the stress in the PZT thick film, caused by the input acceleration [13]. To match the increase in the mechanical damping the electrical damping must be increased accordingly, thus here the optimal resistive load is measured to be higher.

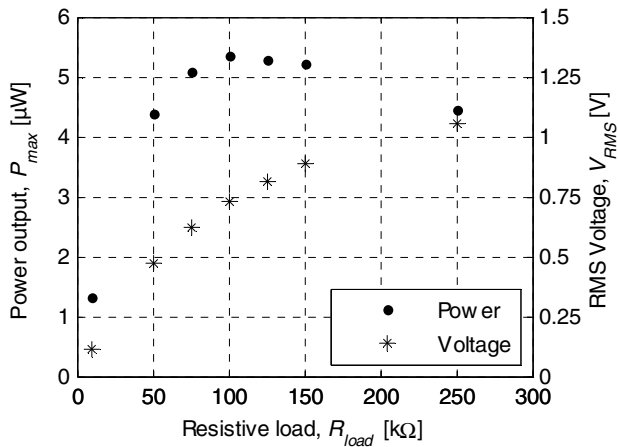


Figure 4: Power output and RMS voltage at resonant frequency as functions of resistive load. Input acceleration is 0.5g.

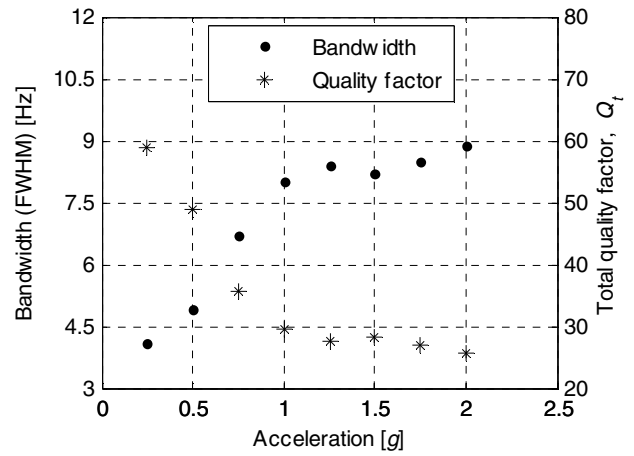


Figure 6: Bandwidth measured as full width at half maximum (FWHM) and total quality factor plotted as functions of input acceleration.

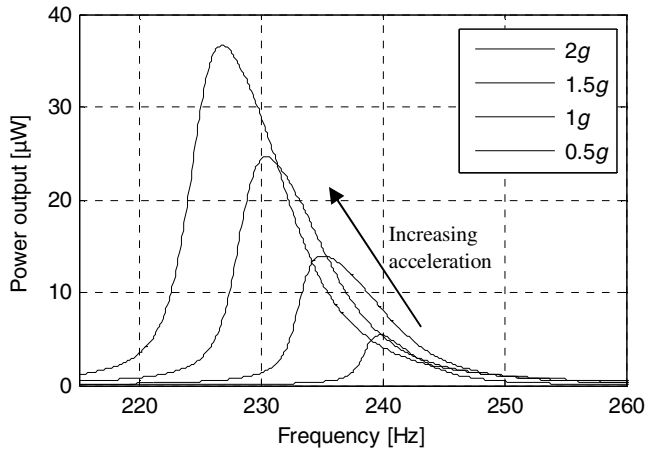


Figure 5: Power output as a function of input frequency for different input accelerations.

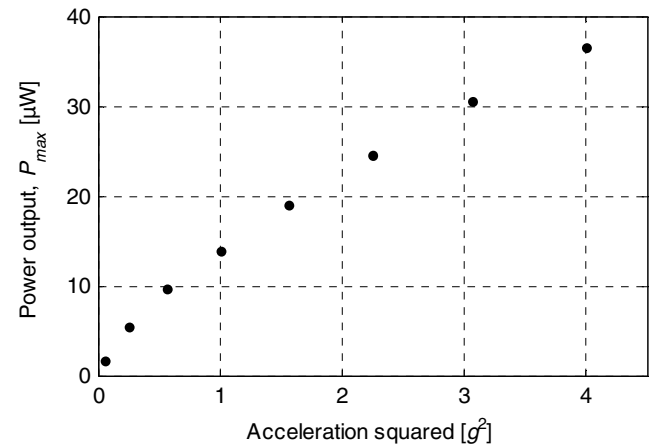


Figure 7: Power output at resonant frequency as a function of input acceleration.

The dissipated power in a resistive load of 100 k $\Omega$  as a function of the frequencies near resonance for different accelerations is shown in Figure 5. A maximum power of 36.65  $\mu$ W is measured at an acceleration of 2g. From Figure 5 it is further seen that the resonant frequency decreases with increasing acceleration. This decrease is due to a non-linear response of PZT under stress. With increasing acceleration, thus stress, the Young's modulus and quality factor decreases [13]. The decrease in Young's modulus will directly reduce the spring constant, thus reduces the resonant frequency. The decrease in quality factor will affect the damping of the system and widen the bandwidth of the resonance peaks, as it is confirmed in Figure 6. The bandwidth in Figure 6 is determined directly from the measurements shown in Figure 5, where the full width at half maximum (FWHM) is defined as the bandwidth. The total quality factor is determined by the ratio between resonant frequency and the bandwidth. Figure 6 shows that with increasing accelerations the total quality factor decreases and the bandwidth increases. The widening of the

bandwidth will lead to a drop in the potential power gain, thus power will no longer have the theoretical quadratic relation with acceleration as expected. This is confirmed in Figure 7 where the power at resonant frequency is plotted for different input accelerations.

## CONCLUSION

A MEMS-based unimorph silicon/PZT thick film vibrational energy harvester with an integrated proof mass has been fabricated and characterized. By defining the 35  $\mu$ m thick cantilevers as the last processing step by the use of KOH etching with a mechanical front side protection it has been possible to obtain a fabrication yield greater than 90%. The resonant frequency of the harvester is aimed towards the common sources of vibrations measured in [14] with resonant frequencies ranging from 100-200 Hz. The unimorph harvester device produces 13.98  $\mu$ W with an optimal resistive load of 100 k $\Omega$  from 1g ( $g=9.81$  m s $^{-2}$ ) input acceleration at its resonant frequency of 235 Hz.

## REFERENCES

- [1] N. S. Hudak and G. G. Amatucci, "Small-scale energy harvesting through thermoelectric, vibration, and radiofrequency power conversion," *Journal of Applied Physics*, vol. 103, no. 10, p. 101301, 2008.
- [2] S. P. Beeby, M. J. Tudor, and N. M. White, "Energy harvesting vibration sources for microsystems applications," *Measurement Science and Technology*, vol. 17, no. 12, pp. R175-R195, 2006.
- [3] Y. Liao and H. A. Sodano, "Model of a single mode energy harvester and properties for optimal power generation," *Smart Materials and Structures*, vol. 17, no. 6, p. 065026, 2008.
- [4] A. Erturk and D. J. Inman, "An experimentally validated bimorph cantilever model for piezoelectric energy harvesting from base excitations," *Smart Materials and Structures*, vol. 18, no. 2, p. 025009, 2009.
- [5] H. Jacobsen, H. Quenzer, B. Wagner, K. Ortner, and T. Jung, "Thick PZT layers deposited by gas flow sputtering," *Sensors and Actuators A: Physical*, vol. 135, no. 1, pp. 23-27, Mar. 2007.
- [6] Qiang Zou, Wei Tan, Eun Sok Kim, and G. Loeb, "Single- and Triaxis Piezoelectric-Bimorph Accelerometers," *Microelectromechanical Systems, Journal of*, vol. 17, no. 1, pp. 45-57, 2008.
- [7] D. Shen et al., "Micromachined PZT cantilever based on SOI structure for low frequency vibration energy harvesting," *Sensors and Actuators A: Physical*, vol. 154, no. 1, pp. 103-108, Aug. 2009.
- [8] R. Lou-Moeller et al., "Screen-printed piezoceramic thick films for miniaturised devices," *Journal of Electroceramics*, vol. 19, no. 4, pp. 333-338, 2007.
- [9] H. Fang et al., "Fabrication and performance of MEMS-based piezoelectric power generator for vibration energy harvesting," *Microelectronics Journal*, vol. 37, no. 11, pp. 1280-1284, Nov. 2006.
- [10] R. Dorey and R. Whatmore, "Electroceramic Thick Film Fabrication for MEMS," *Journal of Electroceramics*, vol. 12, no. 1, pp. 19-32, 2004.
- [11] C. Hindrichsen, R. Lou-Møller, K. Hansen, and E. Thomsen, "Advantages of PZT thick film for MEMS sensors," *Sensors and Actuators A: Physical*, vol. 163, no. 1, pp. 9 - 14, 2010.
- [12] C. C. Hindrichsen, T. Pedersen, E. V. Thomsen, K. Hansen, and R. Lou-Møller, "Investigation of Top/Bottom Electrode and Diffusion Barrier Layer for PZT Thick Film MEMS Sensors," *Ferroelectrics*, vol. 367, no. 1, pp. 201-213, 2008.
- [13] D. Shen, J. Park, J. Ajitsaria, S. Choe, H. C. Wickle, and D. Kim, "The design, fabrication and evaluation of a MEMS PZT cantilever with an integrated Si proof mass for vibration energy harvesting," *Journal of Micromechanics and Microengineering*, vol. 18, no. 5, p. 055017, 2008.
- [14] S. Roundy, P. K. Wright, and J. Rabaey, "A study of low level vibrations as a power source for wireless sensor nodes," *Computer Communications*, vol. 26, no. 11, pp. 1131-1144, Jul. 2003.